ISSN 0036-0244, Russian Journal of Physical Chemistry A, 2007, Vol. 81, No. 12, pp. 1956–1963. © Pleiades Publishing, Ltd., 2007.

CHEMICAL THERMODYNAMICS AND THERMOCHEMISTRY

NMR Shielding and a Thermodynamic Study of the Effect of Environmental Exposure to Petrochemical Solvent on DPPC, an Important Component of Lung Surfactant[1]

M. Monajjemi[a], S. Afsharnezhad[a, b], M. R. Jaafari[c], T. Abdolahi[b], A. Nikosade[b], and H. Monajemi[d]

[a] *Department of Physical Chemistry, Science & Research Branch, Islamic Azad University, Tehran Iran*
[b] *Department of Biochemistry, Mashhad Islamic Azad unisersity of Medical Science, Mashhad, Iran*
[c] *School of Pharmacy, Biotechnology Research Center, Mashhad University of Medical Science, Mashhad, Iran*
[d] *Department of Physics, Islamic Azad University, Karaj, Iran*
e-mail: m_monajjemi@yahoo.com

Recevied February 27, 2007

Abstract—The chemical and petrochemical industries are the major air polluters. Millions of workers are exposed to toxic chemicals on the job, and it is becoming more toxic, causing much damage to respiratory system, today. One of the main components of lung alveoli is a surfactant. DPPC (Dipalmitolphosphatidylcholine) is the predominant lipid component in the lung surfactant, which is responsible for lowering surface tension in alveoli. In this article, we used an approximate model and ab initio computations to describe interactions between DPPC and some chemical solvents, such as benzene, toluene, heptane, acetone, chloroform, ether, and ethanol, which cause lung injuries and lead to respiratory distress such as ARDS. The effect of these solvents on the conformation and disordering of the DPPC head group was investigated by calculations at the Hatree–Fock level using the 6-31G basis set with the Onsager continuum solvation, GAIO, and frequency models. The simulation model was confirmed by accurate NMR measurements as concerns conformational energy. Water can be the most suitable solvent for DPPC. Furthermore, this study shows that ethanol has the most destructive effect on the conformation and lipid disorder of the DPPC head group of the lung surfactant in our model. Our finding will be useful for detecting the dysfunction of DPPC in the lung surfactant caused by acute or chronic exposures to air toxics from petrochemical organic solvent emission source and chronic alcohol consumption, which may lead to ARDS.

DOI: 10.1134/S0036024407120096

INTRODUCTION

The petrochemical sectors of Iran are characterized by a rapid growth of oil demand mainly in the form of gasoline, diesel, liquid field petroleum gas (LPG), and naphtha [1]. The chemical materials that are used in the petrochemical industry are very toxic to humans. Millions of petrochemical workers are exposed to these materials. Petrochemical industry produces air pollutants, and when these air pollutants combine with other pollutants, they become more toxic, causing much damage to respiratory system. Therefore, air pollution is one of the most serious environmental problems in these sectors. It is estimated that millions of people die from these problems every year. One of the important phenomena in the process of respiration is the role of the fluid coating on the walls of the alveoli of the lungs that is called the pulmonary surfactant. The lung surfactant is produced by the alveolar type II cells and is secreted as phospholipid aggregates at the surface of the alveolar membrane.

At the air–water interface, the lung surfactants are adsorbed from the aggregates and form a film [2]. The function of surfactant is to reduce the energy required to inflate lung; it also decreases the likelihood of lung collapse and increases pulmonary compliance [3]. Furthermore, it stabilizes alveoli at low lung volumes and prevents the formation of alveolar edema [4]. Between 90 and 95% of the lung surfactant is made up of lipids, the remainder being proteins [5]. The main component which is responsible for a considerable lowering of interfacial tension is dipalmitoyl phosphatidyl choline (DPPC) which accounts for 50–70% of the PC [6]. DPPC has a gel-to-liquid crystal transition temperature (T_m) of 41.5°C [7].

Therefore, at a physiological temperature of 37°C, it is in the ordered gel state. DPPC contains two saturated acyl chains, it can be tightly packed in the orientated monolayer on the surfactant film. The position of DPPC in the film is determined by its amphiphilic properties. The hydrophilic head group is soluble in the water subphase (Fig. 1), and two acyl chains have hydrophobic interactions with surfactant protein B. The

[1] The article is published in the original.

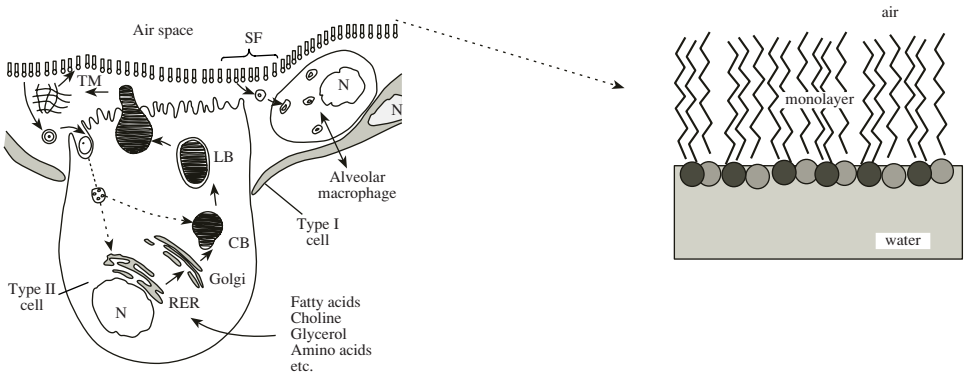

Fig. 1.

dynamic/rheological properties of the DPPC monolayer at small areas per lipid and physiological temperature do not allow for rapid respreading that can follow alveolar space expansion during inhalation (the JMB specific mode of interaction). The SP-B is thought to facilitate the respreading of DPPC [8].

The deficiency and dysfunction of the lung surfactant contribute to the pathophysiology of several severe lung disorders such as respiratory distress syndrome (RDS) and acute respiratory distress syndrome (ARDS) [9]. Several factors appear to increase the risk of ARDS including pneumonia, septic shock, trauma, air pollution, chemical inhalation, cigarette smoking, and alcohol consumption [10].

Air pollutants that enter the respiratory system can potentiate or contribute to respiratory distress. Agents that have received much attention include ozone, nitrogen dioxide, hyperoxia, diesel exhausts, tobacco smoke, silica, and fibrous materials such as asbestos [11]. According to the pervious studies of environmental effects on the extra cellular phospholipids, short exposures to given NO_2 atmospheres (up to 10 ppm) increase the phospholipid content in alveolar washes as the dose and time grow [12]. In another study, it was shown that oxygen atmospheres become critical for the extra cellular surfactant at concentrations above 80%. Under such conditions (80% O_2, 24 h or 100% O_2, 64 h), the amount of phospholipids in lavages decreased as well as the amount of PC and its saturated fraction [13]. Unfortunately, there is less information about chemical materials that alter the conformation of DPPC. Chloroform, ether, benzene, acetone, toluene, heptane, and ethanol are produced in the petrochemical industry in large amounts. All of them pollute the air up to a dangerous level, and they develop faster if they are sprayed.

These carcinogen chemicals can be adsorbed through skin and inhalation. And they can affect respiratory organs. Because these dangerous solutions are vapor, they can travel deeper into the lungs. When these vapors are breathed in, they can irritate and damage the lung causing breathing problems. People who have asthma or some type of lung or heart disease are directly affected by high levels of these solvents. These chemicals found in components of air pollutants can alter pulmonary surfactant DPPC, which may lead to ARDS.

In this article, we discuss the effects of these harmful chemical solvents on surfactant DPPC using the computational simulation method. Recent enhancements in computer power and storage capacities, as well as in computational methods, have led to a rapid evaluation in the field of ab initio NMR calculations. High-resolution nuclear magnetic resonance (NMR) techniques have been widely used to examine rapid isotropic motions of phospholipids dissolved in organic solvents. The nuclear magnetic resonance (NMR) shielding sensor is influenced by several factors, such as molecular structure, temperature, electric gradients and field, and the environment [14].

In the present work, we considered the interaction between the DPPC head group and water molecules in the pulmonary surfactant system and extended our ab initio calculations to determine the minimum energy conformation of the DPPC head group. Furthermore, to explore the effects of solvents on this minimum energy conformation, we performed calculations using the continuum salvation model by Onsager and GAIO. In a single experiment, the chemical shifts of most of the resolved carbons in the DPPC molecule were obtained and compared with the chemical shifts of GAIO calculations.

Our goal was to investigate the effect of chemical inhalation of solvents such as benzene, toluene, heptane, chloroform, ether, and ethanol that could be potential health risks of air pollution cused by petrochemical industry using an ab initio method. These pollutants can change the conformation and ordering of the surfactant DPPC molecule, which leads to ARDS. Our findings will be useful for detecting the dysfunction of DPPC in the lung surfactant caused by acute or chronic exposure to air toxics from an organic solvent emission source that may lead to ARDS.

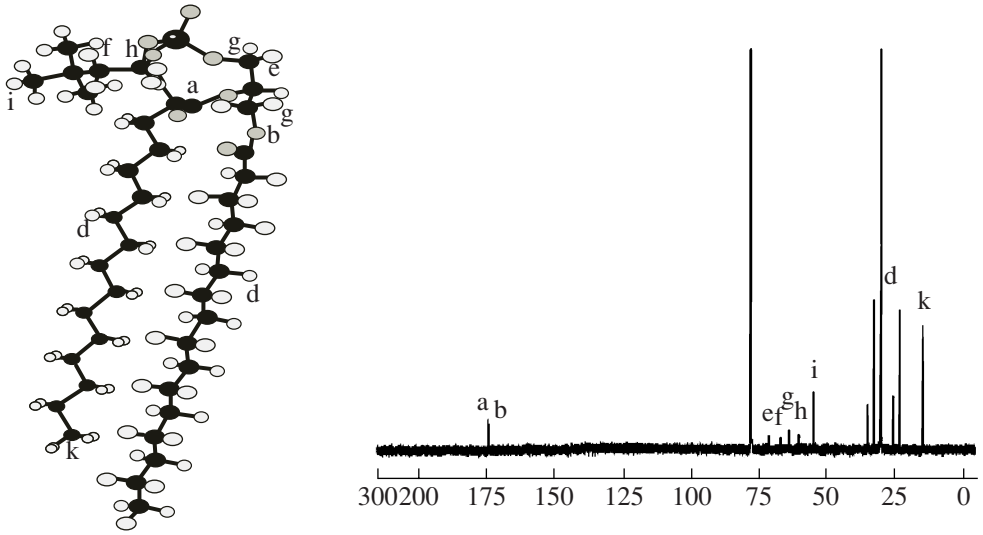

Fig. 2. Plot of the peak position of natural abundance ^{13}C NMR spectra yielding choline and glycerol resonances that are accessible to conformational analysis. Chemical shifts were estimated for the choline C_α (h), C_β (f), and C_γ (i) carbons and for the glycerol C1 (g), C2 (e), and C3 (g) carbons and (a) Sn2–CO and (b) Sn1–CO.

MATERIALS AND METHODS

Pure DPPC was obtained from Avanti Polar Lipids. A chloroform solution of 50 mg DPPC was prepared. After the removal of the solvent, the lipid was hydrated in deuterium oxide under stirring. Small unilamellar vesicles were prepared by sonication using a Branson Sonifier as previously described [15].

Spectroscopic Methods

The ^{13}C-NMR spectra were recorded on a Bruker Avance DRX 500 spectrometer (Fig. 2).

All chemical shifts were referenced to tetramethylsilane. For comparing the results, the chemical shift value (δ) calculated was compared with the results of GIAO calculations (see below). The anisotropic part was determined as $\delta = |\sigma_{iso} - \sigma_{ref}|$.

COMPUTATIONAL METHODS AND THEORY

Ab initio calculations. The GIAO-type methods are invariant with respect to the choice of the gauge for any basis set size [16]. For large molecules and ions, the free energies of solvents obtained by the HF, MP2, and DFT methods are very similar. As far as calculations were concerned, we selected the Hartree–Fock approach and the 6-31G basis set.

The ab initio calculations were carried out using the Gaussian 03 (Revision 3.2) package [17]. The restricted Hartree-Fock (RHF) approach combined with the 6-31G basis set was employed for full optimization of the relevant geometries and then for computations of the corresponding energies and NMR shielding; the latter were evaluated using the coupled Hartree-Fock (CHF) approach and the gauge included atomic orbital (GIAO) method.

Then isotropic part σiso of σ was determined by averaging σ over orientations in the magnetic field, i.e.,

$$\sigma_{iso} = (\sigma_{11} + \sigma_{22} + \sigma_{33})/3.$$

The anisotropy is $\delta = |\sigma_{33} - \sigma_{iso}|$, and the asymmetry is

$$\eta = (\sigma_{22} - \sigma_{33})/\delta.$$

Solvent model. For simulation of a polar environment, the Onsager Self-Consistent Reaction Field (SCRF) model was used as implemented in the Gaussian 03 program. In this model, the solvent is a polarizable medium with a continuous dielectric constant, ε, and the solute forms a cavity in bulk solvent [18]. Partial atomic charges in the polar environment were calculated according to the CHELP charge partitioning scheme. The CHELP (charges from electrostatic potentials) procedure was developed by Chirlian and Francel [19]. In this method, charge is distributed between atoms in a molecule at several thousand points, and the resulting potential is fitted to the electrostatic potential arising from the wave function of the molecule.

Thermochemistry. The geometries at a constant pressure of 1 atm and temperature of 310 K were optimized using the 6-31G basis set, and vibrational frequencies were obtained at the same level. The Gibbs energies were calculated as the energy differences of the solvent for the head group of DPPC by Gaussian 03.

Three equations will be used to derive the final expression used to calculate the different components of the thermodynamic quantities printed out by Gaussian [17].

The partition functions of any component can be used to determine the entropy contribution S for that component using relation (1) from Section 7-6 in [20],

$$n = N/N_A, \text{ and substitute } N_A k_B = R,$$

$$S = R\ln(q(V,T)e) + RT(\partial \ln q/\partial T)_V.$$

The internal thermal energy E can also be obtained from the partition function (2) from Section 3-8 in [20],

$$E = Nk_B T^2(\partial \ln q/\partial T)_V.$$

Ultimately, the energy can be used to obtain the heat capacity (Eq. (3) in Section 3-4 in [20]),

$$C_p(T) = \frac{K(T)\Delta H_{vH}\Delta H_{cal}}{(1 + k(T)^2 RT^2}.$$

RESULTS AND DISCUSSION

The recent studies of the structure and orientation of surfactant DPPC molecules at the air-water interface and the interface between water and an immiscible organic liquid are presented with particular emphasis that DPPC is deposited and the result is a monolayer, a one molecule thick film. Most of the DPPC forming monolayer consists of a polar head group and a nonpolar tail group. The polar head groups are hydrophilic, and therefore "dissolve" in the aqueous layer. The tail groups are hydrophobic and remain on the surface of the subphase. Therefore, in our model, the DPPC head group was connected to solvents. As far as most of the aqueous layer around the head group of DPPC in lung surfactant is water, all of the solvent data were compared with the data on water as a reference solution. All computations were done using the initial geometry reported by Sundaralingam [21]. The obtained theoretical values were compared with the experimental values available (Fig. 3). The initial geometry was compared with the NMR determined structures. In the case of our model (Fig. 4), α_4 = 178.355°, α_2 = 157.354°, α_3 = 72.410°, α_5 = 52.412°, and θ_4 = 52.036° in the gas phase.

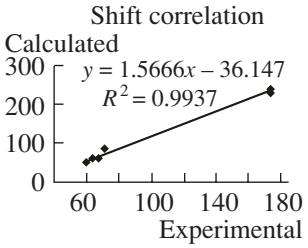

Fig. 3. Comparison between calculated and experimental chemical shifts.

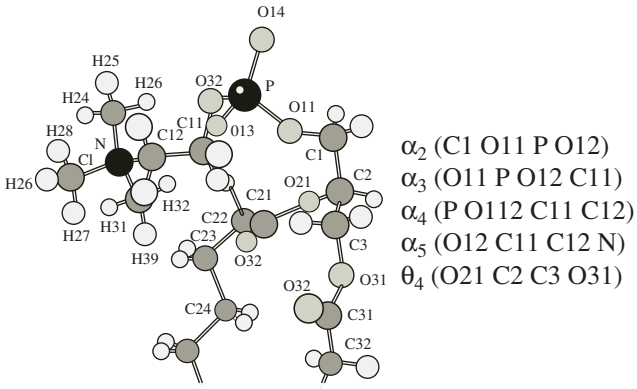

Fig. 4. Atom numbering and notation for torsion angles of the head group DPPC region according to Sundaralingam (1997).

Solvent effects on geometry. Structural molecular properties obtained at the HF/6-31G level were optimized in solvents. DPPC conformer energies in solutions were calculated as the differences between the most stable and most labile conformers. The critical dihedral angles of the DPPC head group in each of the geometries optimized at the same level are shown in Table 1.

All of them were confirmed by the study of Hauser and co-workers, which shows that the PC head group has a distinctly preferred conformation with α_4 in the

Table 1. Dihedral angles of the DPPC head groups optimized at eight dielectric constant values using the Onsager Solvation Model at the HF/6-31G level

ε	α_2, deg	α_3, deg	α_4, deg	α_5, deg	θ_4, deg	ΔE, kcal/mol
78.39	148.690	59.737	172.737	61.523	54.465	0.0
24.55	−173.237	−49.060	−129.858	70.384	57.694	−0.2
20.7	149.102	60.837	172.889	60.653	54.299	−0.7
4.9	−172.281	−48.786	−129.524	70.252	57.925	−3.4
4.335	151.043	64.898	173.746	57.46	53.57	−3.8
2.379	152.751	67.549	174.673	42.206	53.033	−6.1
2.247	152.967	67.841	174.807	56.257	52.98	−6.4
1.92	153.582	68.642	175.199	54.687	52.718	−7.1

Table 2. Enthalpies (ΔH^1, kcal/mol), entropies (ΔS^1, kcal/(mol)), and Gibbs free energies (ΔG^1, kcal/mol) calculated at 310 K and constant pressure from theoretical data

ε	$-\Delta H^1$	$-\Delta G^1$	ΔS^1	$T\Delta S$*	$\Delta G - \Delta H$**
78.39	941520.4515	941576.8005	0.181774	56.34994	56.349
24.55	941520.4515	941576.7955	0.181759	56.34529	56.344
20.7	941520.4509	941576.7986	0.181759	56.34839	56.3477
2.379	941520.4509	941576.7992	0.18177	56.34746	56.3483
4.9	941520.4509	941576.7980	0.181766	56.34653	56.3471
4.335	941520.4509	941576.7967	0.181763	56.3487	56.3458
2.228	941520.4509	941576.7992	0.181771	56.34901	56.3483
1.92	941520.4509	941576.798	0.181768	56.34808	56.3471

range 150°–160° and α_5 ± gauche both in solution and in lipid aggregates [22]. According to Table 1, the relative energies of DPPC head groups also depend on the polarity of the environment. Of all of the solvents, the head group conformer in water (ε = 78) has the lowest energy. Therefore, as concerns conformational energy, water is the most suitable solvent. It may be that, in a polar medium, DPPC conformers become additionally stabilized by intermolecular ionic and hydrogen bond interactions with polar neighboring molecules. Moreover, as the polarity of the medium increases, the conformational stability of this molecule increases faster than in nonpolar solvents. Table 1 also shows that only θ_4 of the dihedral angles is slightly affected by polarity increase, changing from 54.456° (ε = 78.39) to 52.718° (ε = 1.92). Therefore, the dihedral θ_4 angle of this model changes insignificantly as polarity varies, while the remaining geometry parameters are affected. This confirmed that the glycerol backbone is the most rigid part of the lipid head group. All DPPC conformers in nopolar systems have the lowest energy; however, at ε = 78, the difference is only 7.1 kcal/mol.

The dihedral angles α_2, α_3, and α_4 are more sensitive to the medium. Especially, in ethanol and chloroform, these dihedral angles change in opposite directions. Ethanol influences dihedral angles more strongly than chloroform.

The dihedral angle α_2 changes from 148.690° (ε = 78) to 153.582° (ε = 1.92), α_3 changes from 59.737° (ε = 78) to 68.642° (ε = 1.92), α_4 changes from 172.737° (ε = 78) to 175.199° (ε = 1.92), and the dihedral angle α_5 changes in the opposite direction from 61.523° (ε = 78) to 54.687° (ε = 1.92). These results are confirmed by NMR, which also indicates that the significant PC group in aqueous solution has a somewhat increased α_5 torsion angle [22].

Moreover, in comparison with the water phase, the largest dihedral angle change is observed in ethanol.

Solvent effects on electrostatic potential. DPPC contacts the aqueous layer in the lung surfactant. Therefore, it was necessary to determine the electrostatic parameters for nonbonded interactions in the head group region. The electrostatic potential arises from the wave function of the molecule. In this investigation, CHELP charges were used for studying charge variations in the head group region of DPPC in solvents (Table 2).

The CHELP study shows that the largest variations are observed for C21 (Sn1–CO), C31 (Sn2–CO), and phosphorus (Table 3). The phosphorus atom has the lowest charge in water (Fig. 3). Moreover, recent molecular dynamics studies showed that, in the head group region, water molecules were ordered by phosphate, choline, and carbonyl groups. Water molecules form extensive hydrogen bonds with phosphate and carbonyl groups, but do not form hydrogen bonds with the choline group. Therefore, the larger variations of charge of these parts of molecule indicate that the carbonyl plane and phosphorus assume a preferred orientation near the solvent.

DPPC has less charge in benzene (ε = 2.247) compared with the other nonpolar solvents such as toluene, chloroform, ether, and heptane. Because hybridization in benzene makes this molecule more stable than it would be if it had localized bonds.

However, the electrons in benzene are not evenly distributed throughout the molecule. The carbon atoms, which are slightly more electronegative than the hydrogen atoms, pull electrons closer to themselves. Therefore, in comparison with the other noplar solvents, we can see different result of this when we view the benzene electrostatic potential (see Table 3). It seems that variations in the charge electrostatic potential are related to the dielectric constant. Because maximum charges were obtained in nonpolar solvent heptane (ε = 1.92), benzene (ε = 2.247), and toluene (ε = 2.379).

Geometry and frequencies. The geometries of the DPPC head group in each solvent were optimized by the standard ab initio methods using the 6-31G basis set, and vibrational frequencies were obtained at the same level. The Gibbs free energy of the reaction was estimated at 310 K and constant pressure 1 atm for the head group of DPPC using the Gaussian 03 package (Table 2).

Table 3. The charge of DPPC head group atoms in solvents with different dielectric constants

Atom	Dielectric constant							
	78.39	24.55	20.7	4.9	4.335	2.739	2.247	1.92
Cb	−0.2536	−0.25358	−0.25357	−0.25338	−0.25338	−0.253237	−0.254195	−0.253185
N	−0.7783	−0.778215	−0.778203	−0.77792	−0.77784	−0.777484	−0.783497	−0.777322
Ca	−0.2646	−0.264617	−0.264624	−0.26463	−0.26466	−0.264438	0.265515	−0.264297
Cc	−0.2734	−0.27307	−0.273002	−0.27189	−0.27175	−0.271039	−0.230583	−0.270863
C12	−0.1094	−0.109073	−0.108971	−0.10727	−0.10703	−0.10575	−0.106281	−0.105234
C11	0.06138	0.061216	0.061183	0.061232	0.061037	0.061222	0.060858	0.061439
O12	−0.9159	−0.916665	−0.91687	−0.92062	−0.92106	−0.923925	−0.924177	−0.925145
P	1.95925	1.959972	1.960158	1.96294	1.96339	1.96534	1.965631	1.96612
O14	−0.8741	−0.874375	−0.87445	−0.8753	−0.87551	−0.875918	−0.875973	−0.876029
O13	−0.9202	−0.920315	−0.920339	−0.92086	−0.92081	−0.920901	−0.92091	−0.920878
O11	−0.945	−0.944445	−0.944306	−0.94168	−0.94146	−0.939645	−0.939508	−0.938908
C1	−0.5518	0.054721	0.054605	0.052331	0.052126	0.050322	0.050164	0.04953
C2	−0.16234	0.162821	0.16295	0.165299	0.165579	0.167643	0.166246	0.168541
O21	−0.7577	−0.757923	−0.757988	−0.75895	−0.75913	−0.759898	−0.756223	−0.760173
C21	−0.87682	0.876732	0.876712	0.876749	0.876578	0.876316	0.874026	0.876162
O22	−0.66	−0.659965	−0.659965	−0.66046	−0.66038	−0.660848	−0.660893	−0.611065
C22	−0.4048	−0.404922	−0.404946	−0.40535	−0.4054	−0.405538	−0.40549	−0.405601
C3	−0.02377	0.023888	0.02391	0.024174	0.024222	0.024312	0.02435	0.024315
O31	−0.7341	−0.734034	−0.73401	−0.73369	−0.73363	−0.733383	−0.733338	−0.733278
C31	−0.78962	−0.790018	0.790117	0.791862	0.792049	0.793303	0.79351	0.793831
O21	−0.6046	−0.604684	−0.604714	−0.60511	−0.60516	−0.605495	−0.605652	−0.605639
C23	−0.4499	−0.44992	−0.449912	−0.44972	−0.4497	−0.449695	−0.449711	−0.449694
C32	−0.516	−0.51599	−0.515998	−0.51606	−0.516	0.515927	−0.515943	−0.515905
H24	0.21136	0.211302	0.211287	0.210983	0.210947	0.210612	0.21054	0.210451
H25	0.21365	0.213723	0.213744	0.214135	0.214186	0.214582	0.214638	0.2148
H26	0.21162	0.21135	0.211286	0.210155	0.209987	0.209146	0.209	0.208797
H27	0.34283	0.342956	0.34298	0.343271	0.343259	0.34331	0.343272	0.343214
H28	0.18714	0.186604	0.186467	0.18425	0.183952	0.182283	0.182088	0.181557
H29	0.19313	0.193638	0.193767	0.195987	0.196297	0.198108	0.198298	0.199007
H30	0.32253	0.322521	0.322518	0.321997	0.321959	0.320631	0.307859	0.319821
H31	0.20726	0.208241	0.208501	0.213315	0.213914	0.218358	0.209381	0.220595
H32	0.19977	0.199269	0.199135	0.196686	0.196402	0.194263	0.184576	0.19324

The entropy was evaluated by the standard statistical thermodynamics methods,

$$\Delta S = \Delta H_{\text{cal}}/T_m.$$

According to Table 2, the most negative Gibbs free energy of DPPC was obtained in water, as also follows from Table 1. And also, ethanol is the less favorable solvent for DPPC because it has a lower entropy and higher Gibbs free energy.

For comparing the results, the entropy data are given as obtained by the standard statistical thermodynamics method; the $T\Delta S$ (T) values were calculated by the equation $G = H - T\Delta S$ from our data. We see that the $\Delta G - \Delta H$ calculated values are about 0.0008 kcal/mol.

Calculation of NMR parameters in the solvent model. The Gauge Including Atomic Orbital (GIAO) approach was used. The ab initio GIAO calculations of NMR chemical shielding tensors were performed using the SCF Hartree–Fock approximation. The chemical shielding tensors were calculated with the Gaussian 03 program. At each dielectric constant, the nuclear shielding was calculated for each geometric structure (Table 4). These data were compared with the result obtained from the 13C NMR spectra of DPPC. These

Table 4. 6-31G calculations of the $\langle\sigma_{iso}\rangle$ in ppm and the nuclear magnetic shielding tensor σ for some carbon atoms

ε	$\langle\sigma_{iso}\rangle$	Δσ	$\langle\sigma_{iso}\rangle$	Δσ	$\langle\sigma_{iso}\rangle$	Δσ	$\langle\sigma_{iso}\rangle$	Δσ
	Ci(a)		C12		C11		C21(Sn2–CO)	
78.39	155.491	32.619	146.5344	7.3153	155.6538	0.4501	13.5071	84.6973
24.55	155.384	32.8455	146.623	7.7358	155.714	0.2243	13.4479	85.2017
20.7	155.356	32.9036	146.6436	7.8482	155.7297	0.1608	13.4319	85.3284
4.9	154.8864	33.7999	146.9949	9.8102	155.9811	1.0574	13.1122	87.3656
4.335	154.8122	33.9478	147.0367	10.0547	156.0159	1.2225	13.0738	87.6109
2.379	154.433	34.4469	147.241	11.7006	156.195	2.3709	12.7721	89.0559
2.228	154.3908	34.5009	147.2612	11.9069	156.2116	2.513	12.7356	89.203
1.92	154.2693	34.6213	147.3219	12.4876	156.2573	2.9351	12.6335	89.6752
	C1		C2		C3		C31(Sn1–CO)	
78.39	148.6915	13.9064	132.5199	29.2304	148.1804	5.1853	19.5317	64.5142
24.55	148.705	13.8533	132.521	29.2391	148.175	5.2138	19.5438	63.8668
20.7	148.7084	13.8382	132.5217	29.2417	148.1737	5.2209	19.5472	63.6925
4.9	148.8007	13.5972	132.5399	29.2915	148.1589	5.3263	19.5949	60.4908
4.335	148.808	13.5526	132.5335	29.3088	148.1637	5.329	19.6071	60.1238
2.379	148.905	13.2843	132.52	29.3993	148.12	5.4195	19.6016	57.4437
2.228	148.9171	13.2447	132.5183	29.4133	148.1186	5.4231	19.6011	57.1436
1.92	148.9524	13.1322	132.5207	29.4438	148.101	5.4485	19.5928	56.2226

data were identical with the result obtained from the 13C NMR spectra of phosphatidylcholines, and it was confirmed that chemical shift anisotropy varied most strongly in the choline group of the head region. In order to compare the calculated chemical shifts with experimental, it is important to use consistent nuclear shielding for NMR reference compounds like TMS. For standard TMS, we obtained in this work for the minimum energy conformation 208.04 against the literature and experimental values 195.1 and 188.1, respectively [23].

CONCLUSIONS

Unfortunately, a large number of treatments of ARDS failed to improve survival. The medicines used included glucocorticosteroids, surfactants, prostaglandin El, ketoconazole, prostacyclin, nitric oxide, and almitrine [24]. Since there is no specific treatment, the identification of patients with a higher risk of the development of ARDS is of paramount importance. Therefore, more fundamental understanding of lung surfactant functions (surfactant alternations contribute to ARDS) can inspire the hope of controlling this once fatal disease. We therefore used a very approximate model to describe the interactions between DPPC as an important component of the lung surfactant and some solvents, since lung surfactant changes may lead to pulmonary diseases such as ARDS.

We chose our model of DPPC because it was the most common biological lipid in the lung surfactant. And there are few data on the effects of pollutants on DPPC.

Over the past three decades, ab initio quantum chemistry has become an essential tool in the study of molecules and, increasingly, in modeling complex systems such as those arising in biological science. In this investigation, molecular modeling by Gaussian 03 was used to investigate the effect of a series of pollutants, some of which may cause changes in surfactant phospholipids mainly in DPPC.

The simulation model was confirmed by accurate NMR measurements experimentally. According to the CHELP and conformational energy results, electrostatic force variations are related to the dielectric constant. The DPPC head group in water had the lowest polarization and the highest stability. However, the results of dihedral angle and thermochemisty calculations by the frequency method showed that the strongest conformation and lipid head group disorder variations were those in ethanol and chloroform. In general, the effect of harmful solutions in air depends on the solubility of reactive chemicals in aqueous media. In our investigation, ethanol in comparison with the other solvents is best soluble in water, which is also absorbed by the upper respiratory tract and thus occurs in very low concentrations in the bronchiolar and alveolar regions. Ethanol molecules that penetrate into the lower respiratory tract are mostly vapor forms of pollutants, or are adsorbed on other components, such as small particles of aerosols. When these vapors are breathed in, they can affect the lung and cause breathing problems. There-

fore, they can defect the function of DPPC in the lung surfactant. According to experiments, alcohols have a destabilizing action on model membranes [25]. It was observed that, upon the addition of alcohols, the lipid bilayer became thinner and the area per molecule increased. The calculated increase in area/molecule was confirmed by flow experiments where bilayers of aspirated vesicles were seen to laterally expand upon the exposure to aqueous streams containing ethanol. The reduction in the interfacial tension of a bilayer by ethanol is much smaller than can be predicted by simply making a direct comparison with the behavior of an alkane such as heptane.

To summarize, this work shows that ethanol has the strongest effect on the DPPC head group of the lung suractant in our model. DPPC forming a monolayer consists of a polar head group and a nonpolar tail group. The tail groups are hydrophobic and remain on the surface of the subphase. As the monolayer is compressed, the hydrophobic tails alter their positions. Different configurations of molecules on the surface can be distinguished by the behavior of surface pressure during monolayer compression. Various configurations of hydrocarbon chains affect the head group DPPC region. Therefore, the behavior of hydrophobic tails should be considered. Furthermore, the results obtained should be evaluated against experimental data on animal models.

Finally, our findings will be useful for detecting dysfunction of DPPC in the lung surfactant due to ADRS risks of acute of chronic exposures to air toxics from petrochemical organic solvent emission source and chronic alcohol consumption. And also, we wish to point out the potential of this analysis for further studies of molecular modeling of the lung surfactant. The effects of these solvents in the hydration model of the monolayer membrane of the lung surfactant with SP proteins should be considered.

REFERENCES

1. Homa Keshavarzi Shirazi and Mohsen Mir Mohamadi, Indoor Built Environ. **13**, 295 (2004).
2. C. Vermehren, S. Frokjaer., and J. Hansen, Int. J. Pharm. **307**, 89 (2006).
3. B. Müller, C. Seifart, and P. J. Barth, Eur. J. Clin. Investigat. **28**, 762 (1998).
4. R. J. Mason, MD, J. Med. **143**, 611 (1985).
5. C. S. Gross, P. J. Simms, R. W. Townec, and R. E. Mi., J. Chromatogr., B: Biomed. Appl. **744**, 407 (2000).
6. Annette Gulik, Pierre Tchoreloff, and Jacques Proust, Biophys. J. **67**, 1107 (1994).
7. Heejung Yun, Young-Wook Choi, Nam Jeong Kim, and Daewon Soh, Bull. Korean Chem. Soc. **24** (3), 377 (2003).
8. Gang Ma and H. C. Allen, Langmuir **22**, 5341 (2005).
9. L. Hawkes and H. M. Ulla, Hospital Pharm. Respir. Res. **3**, 14 (2002).
10. E. C. Iribarren, D. R. Jacobs, Jr., M. D. Gross, et al., *Cigarette Smoking, Alcohol Consumption, and Risk of ARDS: A 15-Year Cohort Study in a Managed Care Setting*, Chest **117**, 163 (2000).
11. Back SO and Jenkins RA, Indoor Built Environ. **10**, 200 (2001).
12. B. Müller, C. Seifart, and P. J. Barth, Eur. J. Clin. Investigat. **28**, 762 (1998).
13. J. L. Malloy and A. Ruud., Appl. Physiol. **88**, 401 (2000).
14. J. A. Tossel, *Nuclear Magnetic Shielding and Molecular Structure* (Kluwer Academic, Amsterdam, 1993).
15. L. D. Mayer, M. J. Hope, and P. R. Cullis, Biochim. Biophys. Acta **858**, 161 (1986).
16. I. Ando and G. A. Webb, *Theory of NMR Parameters* (Academic, London, 1983).
17. M. J. Frisch, G. W. Turcks, H. B. Schlegel, et al., *Gaussian 03* (Gaussian, Inc., Pittsburgh, PA, 2003).
18. J. Landin and I. Pascher, J. Phys. Chem. A. **101**, 22996 (1997).
19. Y. Albert and L. A. Benesch, Can. J. Chem. **72**, 1596 (1994).
20. D. A. McQuarrie and J. D. Simon, Molecular Thermodynamic (1999).
21. M. Sundaralingam, Ann. N. Y. Acad. Sci. **195**, 324 (1972).
22. H. Hauser, I. Pascher, R. H. Pearson, and S. Sundell, Biochim. Biophys. Acta **650** (1), 21 (1981).
23. M. Baaden, P. Granger, and A. Strich, Mol. Phys. **98**, 329 (2000).
24. F. Kahdi, M. D. Udobi, and M. D. Ed Childs, Am. Fam. Physician **67**, 315 (2003).
25. J. A. Barry and K. Gawrisch, Biochemistry **33** (26), 8082 (1994).